A Comparative Study Between Transformer Coupled Un-Tuned and Tuned Power Derivative Circuits for Ultrasonic Cleaning System

S. M. A. Motakabber*, Md. Mominul Hoque, and A. H. M. Zahirul Alam

Dept. of Electrical & Computer Engineering, International Islamic University Malaysia, Kuala Lumpur, Malaysia

*Corresponding author: amotakabber@iium.edu.my

(Received: 20 June 2024; Accepted: 25 September 2024)

Abstract— This paper discusses the challenges in developing a high-efficiency driver circuit for an ultrasonic cleaning system. The main issue lies in finding the suitable driver circuit and drive signal to ensure the correct frequency level for the ultrasonic transducer. This difficulty affects the removal of contaminants from inaccessible areas due to the inability to control cavitation bubbles. To address these problems, the authors studied the behaviour of piezoelectric transducers and designed driver and output power circuits. The LTspice XVII software was used to design and simulate various circuits, and it was found that trapezoidal pulses were the most suitable drive signals for avoiding power loss and achieving reasonable efficiency. The generated output frequency of 38.6 kHz provides sufficient energy for cleaning various small metallic items like jewellery, wristwatches, glasses, etc. The findings of this study will be helpful for those conducting research in this area in the future.

Keywords: *Ultrasonic, Piezoelectric Effect, Ultrasonic Transducer and Megasonic Transducer.*

1. INTRODUCTION

Ultrasonic cleaning systems use sound waves generated by converting mechanical energy into electrical energy. The frequency of these waves ranges from 20 kHz to 170 kHz and depends on the specific application. A typical system consists of a tank filled with a liquid solvent, cleaning items, and a driver circuit or ultrasonic vibration generator. The driver circuit drives a piezoelectric transducer, which produces the ultrasonic waves. The design of the circuit can vary, but the ultimate goal is to create cavitation bubbles, which are essential for removing contaminants from the items. A basic block diagram of an ultrasonic cleaning system is shown in Fig. 1.

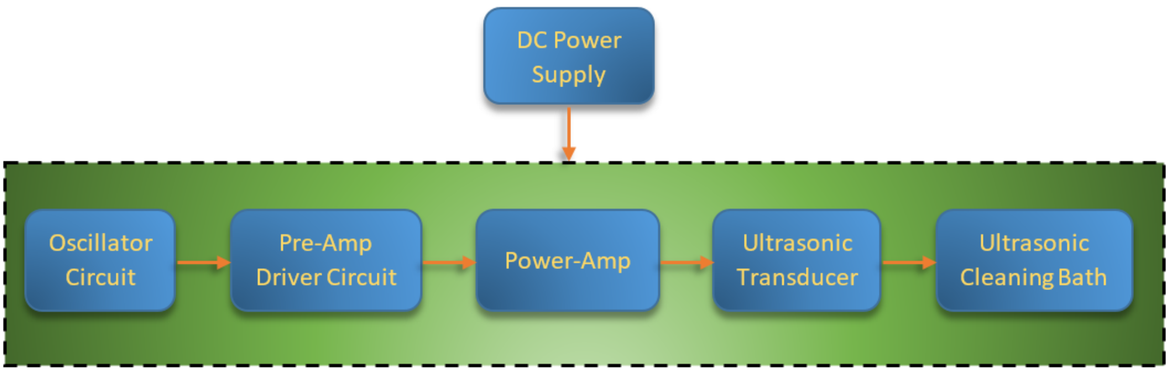

Fig. 1 Basic block diagram of an ultrasonic cleaning systems

In general, an electrical generator, an ultrasound transducer and a cleaning solvent tank are the fundamental

DOI: https://doi.org/10.69955/ajoeee.2024.v4i2.59

elements of an ultrasonic cleaning system. The leading tank designs in the business are heavy-duty, with a range of shapes and sizes ranging from 1 to 200 gallons, all in stainless steel. However, as time passed with technology evolution, many researchers in the field of electronics have performed studies to enhance the performance of ultrasonic cleaning, in which their testing methods focus on the nature of power circuits, controls and optimum frequency of activity for ultrasonic cleaning systems. The historical overview of ultrasonic cleaning traces its origins to the early 20th century. It highlights the pivotal role played by Paul Langevin's invention of the Langevin transducer in 1917, which laid the foundation for subsequent research and development in ultrasonic applications. The concept of sonochemistry, introduced by Wood and Loomis in 1927, further solidified the scientific understanding of ultrasonic cleaning and its underlying mechanisms. The emergence of the system can be seen to revive around the 1950s when several companies in the USA and UK started to develop and utilize it in their factory for unknown reasons [1].

In earlier systems, items were cleaned in a multi-tank process involving chlorinated solvents, pre-washing, and ultrasonic cleaning. Today, the cleaning process is typically streamlined, with contaminated items directly immersed in a solvent tank for complete cleaning, including cavitation. While the basic steps remain similar, advancements in solvents and operational frequencies have improved efficiency and effectiveness.

Traditional cleaning methods are used in various industries, including the heavy industry, food industry, medical instruments, clothing, and textiles. These methods often involve using hot solvents, detergents, or pressurized jets to remove contaminants [2]. However, many of these methods have limitations, such as environmental concerns associated with chlorinated solvents or the need for additional sterilization steps in medical applications.

The difference between ultrasonic and Megasonic cleaning is their frequency ranges. Ultrasonic cleaning typically operates between 25 and 270 kHz, while megasonic cleaning uses frequencies between 430 and 5 MHz [3]. It has a noticeable impact on the fluids. Random cavitation happens throughout the cleaning solution for ultrasonic washing since it requires lower frequencies, which later will automatically allow the cleaning force to reach all of the manually inaccessible areas. In comparison, the high frequencies of Megasonics induce fluid motions that contribute to stable cavitation without implosion, which differs from ultrasonic, where the cavitation is transient or cyclical. This implies that the cleaning happens in a line-of-sight manner, allowing only the side of the portion in front of the transducer to be cleaned [4]. The lower frequencies of ultrasonic cleaning are more suitable for general cleaning applications, while megasonic cleaning is often used for precision cleaning tasks, particularly in the electronics industry.

Ultrasonic cleaning applications are wide as they compromise the cleaning of dentures, 3D printing, textiles and many others. Even though higher frequency positively affects cleaning quality, the frequency of ultrasonic is not something to belittle. According to [5], the industrial ultrasonic cleaning frequencies are usually 20 kHz to 80 kHz, as frequencies beyond 100 kHz are suitable for precision cleaning. Megasonics, on the other hand, are particularly helpful in extracting sub-micron particles from flat surfaces. It is typically used mainly in the electronics industry to prepare silicon wafers at a relatively low risk of substrate impact. Fig. 2 shows the graphic comparison between ultrasonic cleaning and Megasonics cleaning.

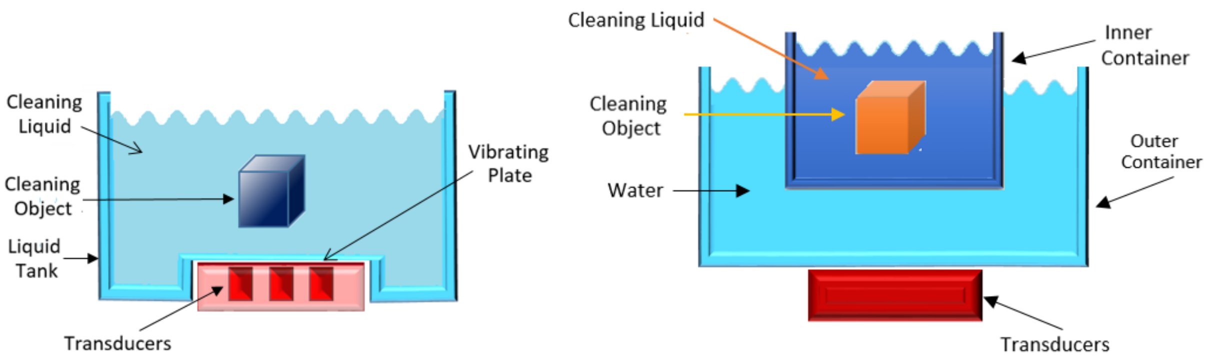

Fig. 2 The cross-section of (a) ultrasonic cleaning and (b) Megasonics cleaning [6]

An Ultrasonic Smart Cleaning Device (UCD) system proposed by Duran and Teke [7] that operates cleaning time independently to save resources and ensure healthy cleaning has been suggested. The system composition comprises four parts: the cleaning tank, ultrasonic transducer, inverter, and fluid analysis circuit. The conductivity and turbidity sensors are mounted with the container. These sensors submit data to the controller circuit encompassing two divisions, each with its microcontroller. The first microcontroller collects data from the sensors, such as the used liquid's temperature, conductivity, and turbidity. The algorithm tracks fluid changes and measures the cleaning period by regulating the fluid solution. Fig. 3 shows the block diagram of the overall system.

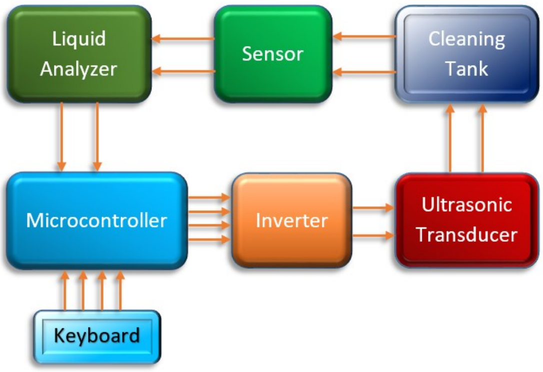

Fig. 3 Control system block diagram of UCD

The first section of the controller circuit involves an inverter system and an algorithm for temperature control. A full-bridging circuit of high frequencies was introduced to drive the ultrasound transducer for cavitation bubble generation. The microcontroller sets the operating frequency of the piezoelectric transducer to 38k Hz. The first microcontroller would then transfer data to another microcontroller to decide on the run period. The second microcontroller decides the cleaning process or works on the user interface. This overall process works dynamically with the help of software implementation.

Athira and Deepa presented a solar-powered ultrasonic cleaner with a twofold mode, charging and discharging [8]. The technique used is the multi-output half-bridge converter and a parallel-fed resonant inverter. The main objective here is to minimize part sizes so that they apply to low-power induction heating. Overall, this system can generate 230V voltage at 28 kHz. For load management purposes, the PI device is implemented. Lead acid batteries in converters are desirable for charging because they are cost-effective [9]. The proposed integrated system of this solar ultrasonic cleaning is shown in Fig. 4.

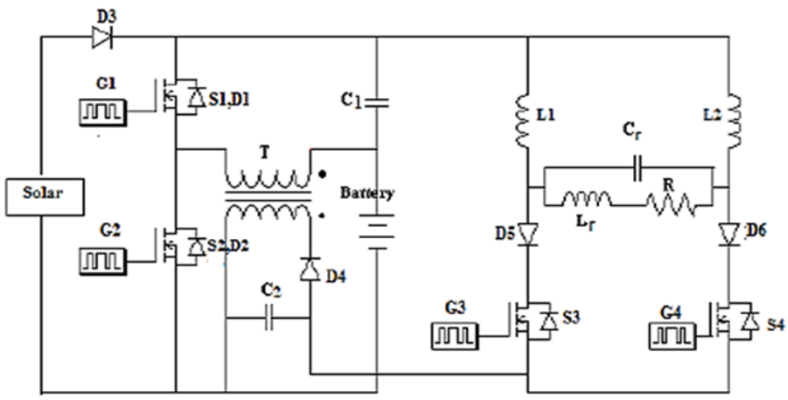

Fig. 4 Integrated system of solar-powered ultrasonic cleaner [9]

In [9], a Varying Frequency Ultrasonic Amplifier [10] offers the configuration of the amplifier with various frequencies. This amplifier system comprises transformers, bridge rectifiers, signal generators and a driver circuit consisting of a pre-amplifier and H-bridge. The signal generator, pre-amplifier and transducer are operated by a $220V_{AC}$ supply.

In [11], an incorporates redesigning the current Phase Controlled Thyristors (PCT) circuit to expand the operational range using impedance characteristics. In general, the system is composed of a few parts. First, the full-bridge rectifier converts the AC to DC voltage with a capacitor filter that filters the ripple voltage. A class-D inverter with two power switches as MOSFETs functions to convert back the DC voltage to AC voltage at a high switching frequency. While the series inductor extends the output voltage across the PCT load, signal conditioning is needed to detect output and input current, and finally, the ultrasonic cleaner and microcontroller. The configuration of the system can be seen in Fig. 5.

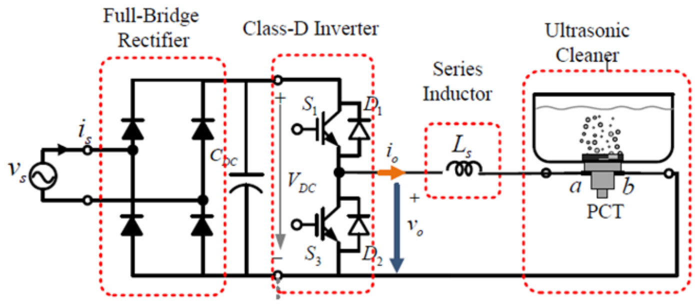

Fig. 5 A class-D inverter configuration system source [11]

2 OUTPUT POWER DRIVE CIRCUIT

A step-up transformer was used where the turns ratio (TR) of secondary to primary can be obtained from the transformer energy equations Eq. (1) to Eq. (3). For simplicity, the transformer was considered an ideal transformer. So, the amount of energy supplied to the transformer's primary is equivalent to the power delivered to the secondary of the transformer.

$$\frac{1}{2}(L_P)(I_P)^2 = \frac{1}{2}(L_S)(I_S)^2 \tag{1}$$

$$\sqrt{\frac{L_S}{L_P}} = \frac{I_P}{I_S} = \frac{V_S}{V_P} = \text{TR} \tag{2}$$

$$\text{TR} = \frac{N_2}{N_1} = \sqrt{\frac{L_S}{L_P}} \tag{3}$$

Where, L_P, I_P, V_P, N_P are the transformer's primary coil inductance, current, voltage, and number of trans coils, respectively. Similarly, L_S, I_S, V_S, N_S are the transformer secondary coil inductance, current, voltage and number of trans of the coil, respectively.

2.1 H-Bridge Circuit and Piezoelectric Transducer

The purpose of including an H-bridge circuit is to drive sufficient energy to the ultrasonic transducer. In the proposed circuit, MOSFETs of type IRFZ44N have been used due to their characteristics, which are low in resistance and can drive more power. The parameters and the design model of the piezoelectric transducer used the values of parallel capacitance, $C_d = 2430pF$, series inducatance $L_s = 110.83mH$, series resistance $R_s = 333.7\Omega$ and series capacitance $C_s = 153.4pF$ respectively.

3 OUTPUT POWER DRIVE CIRCUIT

Two types of arrangements were used for the transformer drives output circuit, namely untuned and tuned transformer circuits. To further understand the differences between these two circuits, the block diagram of both the untuned step-up transformer circuit and tuned secondary step-up transformer circuit can be seen in Fig. 6(a) and Fig. 6(b), respectively, where the red boxes and remarks indicate parts that have undergo iteration.

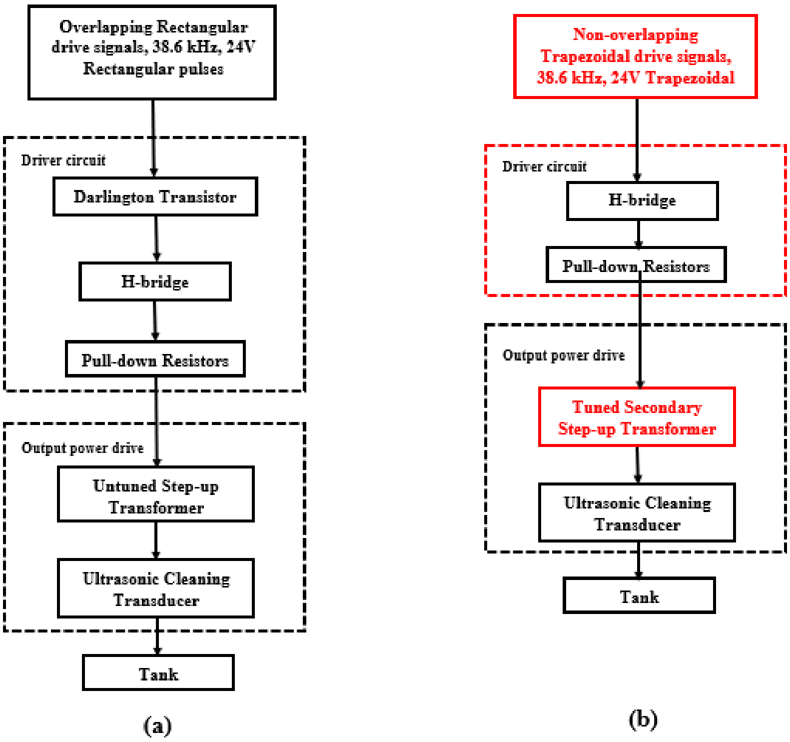

Fig. 6 Block diagram of the transformer circuit (a) untuned and (b) tuned secondary

3.1 Untuned Step-Up Transformer Circuit

The circuit shown in Fig. 7 is the overall circuit to be adapted in the ultrasonic cleaning system, where it comprises two primary sections: the driving circuit and the output power drive circuit. Areas outside the dotted red box indicate the driving circuit part, which includes a Darlington transistor, a pair of pull-down resistors, an H-bridge circuit containing four MOSFETs and also two voltage sources that drive them, which are a signal voltage drive and a power supply voltage. Meanwhile, areas included inside the dotted red box are the output power drive circuit that consists of a step-up transformer and an ultrasonic transducer. If a prototype is built, this part will be connected to the cleaning tank.

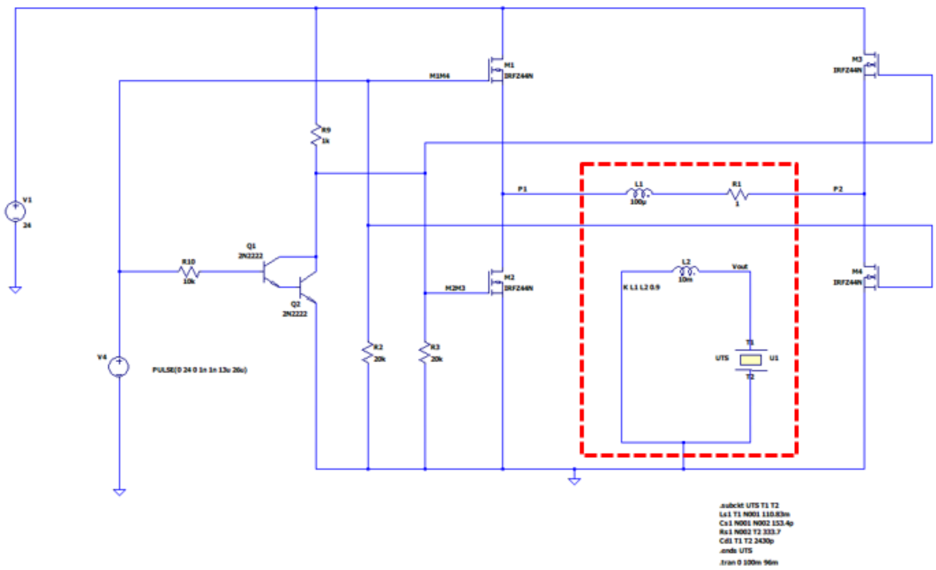

Fig. 7 Untuned step-up transformer circuit

3.2 Tuned Secondary Step-Up Transformer Circuit

The circuit shown in Fig. 8 results from iterations after a few changes on the driving circuit and ultrasonic cleaning system sections have been made on the previous circuit. On the driving circuit part, no changes were made to the power output except for the Darlington transistors, which were removed with their load and base resistors. Meanwhile, the secondary coil of the step-up transformer in the ultrasonic cleaning portion was tuned by adding a parallel capacitor. The idea was to isolate the inductances of the secondary from interfering with the transducer load and the calculation of the parallel capacitor. It can be seen that the areas outside the red box are the driver circuit, which is comprised of an H-bridge circuit and pull-down resistors. In contrast, the dotted red box includes the output power drive circuit comprising a tuned secondary step-up transformer and transducer.

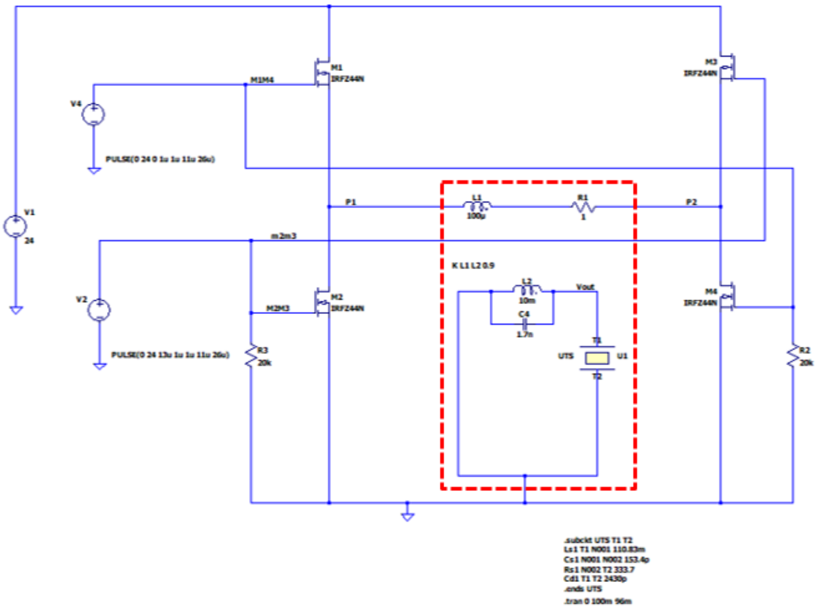

Fig. 8 Equivalent circuit of tuned secondary step-up transformer circuit

4 RESULT

4.1 Untuned Step-up Transformer Circuit

In order to compute the efficiency of the circuit, the power loss occurring at R1 and MOSFETs were recorded where the drain and source currents of MOSFETs during switching transitions were the power lost dissipated across Rd_{on}. Fig. 9 shows the output waveform of the driving transformer. The peak current through the drain and source of MOSFETs were obtained, as shown in Fig. 10(b). Also, for efficiency calculation, the current through the load was also recorded to compute the power dissipated across the resistive component of the transducer, Rs. In Fig. 10(c), it can be observed that an overlap switching occurs at the voltage of V(m2m3) and V(m1m4). It was assumed the pulse was triangular. Even though, based on Fig. 10, the output frequency of the system is recorded to be at 38.6kHz, based on the calculations, the efficiency rate of the circuit is 35.10%, which is quite unsatisfactory to be adapted to real-life adaptation.

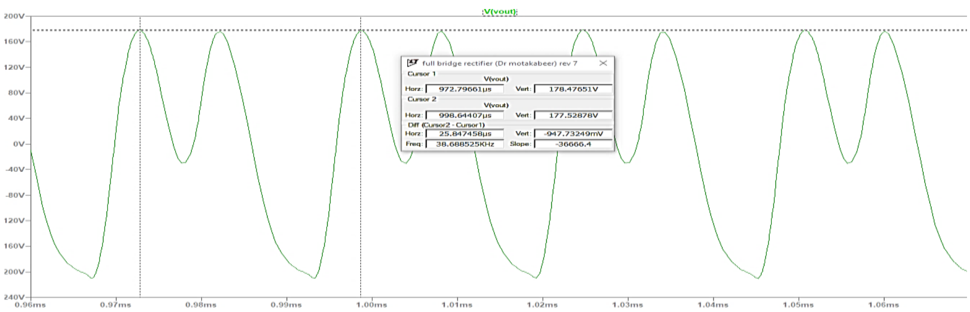

Fig. 9: The oscillation frequency waveform of the system

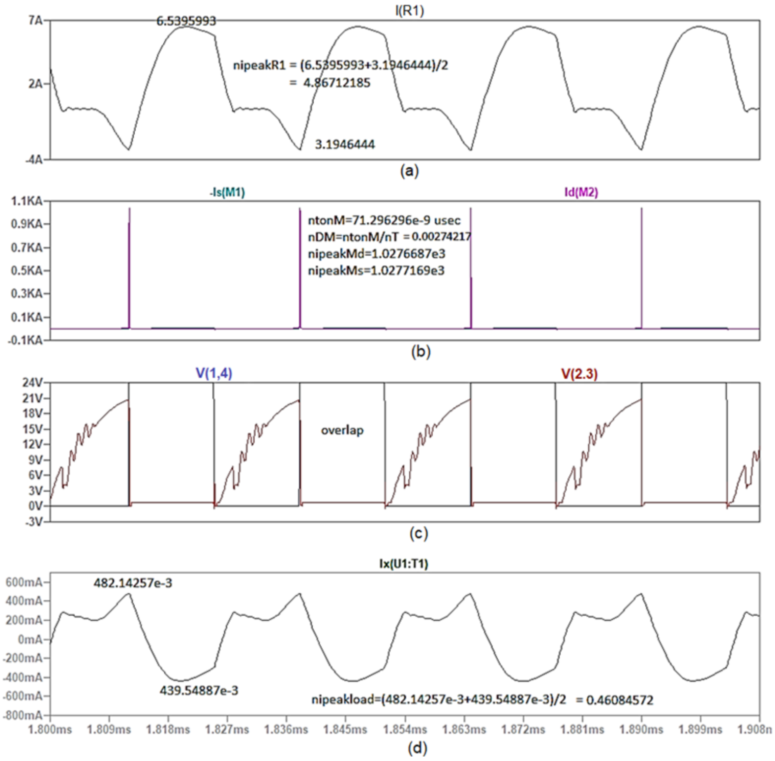

Fig. 10: The output waveforms for un-tuned transformer circuit, (a) current in R1, (b) current in MOSFET, (c) voltage at V(1,4) and V(2,3) and (d) current at the load

4.2 Tuned Secondary Step-up Transformer Circuit

The output waveforms generated from the tuned secondary step-up transformer circuit are shown in Fig 11, where four different readings have been analyzed. The technique previously used in the un-tuned step-up transformer circuit has also been adapted to compute the circuit's efficiency. The power loss occurring at R1 and MOSFETs were recorded where the drain and source currents of MOSFETs during switching transitions where the power lost dissipated across Rd_{on}. The peak current through the drain and source of MOSFETs were obtained, as shown in Fig. 12(b). In Fig. 12(c), it is observed that the trapezoidal signal has eliminated the overlapping scenario that once happened at the voltage of V(1,4) and V(2,3) in the previous circuit. Based on the calculations, it can be seen that this tuned secondary step-up transformer circuit was established operational at a reasonable efficiency of 70.51%. Also, based on Fig. 12, it has an output frequency of approximately 38.6 kHz, thus making it a better option to be adapted in the real-life ultrasonic cleaning system. A comparative analysis between the two circuits can be made based on a few significant parameters summarized in Table 1.

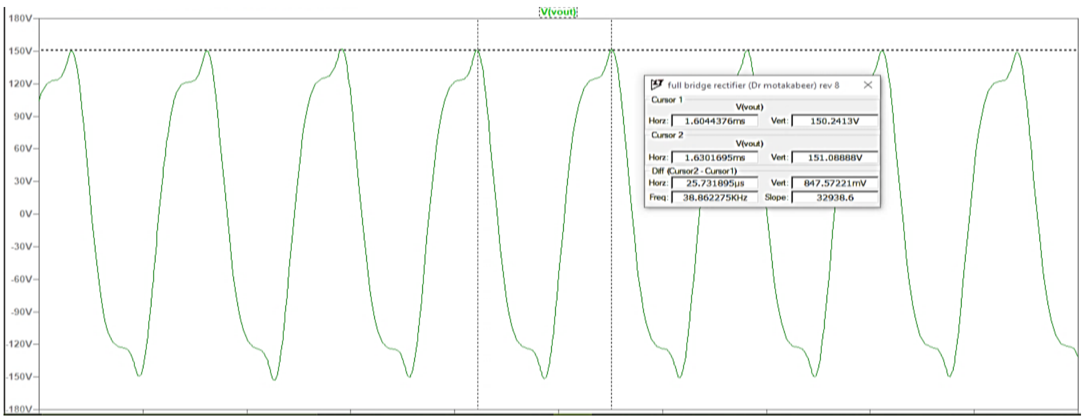

Fig. 11 The output frequency of the Tuned Secondary Step-up Transformer circuit

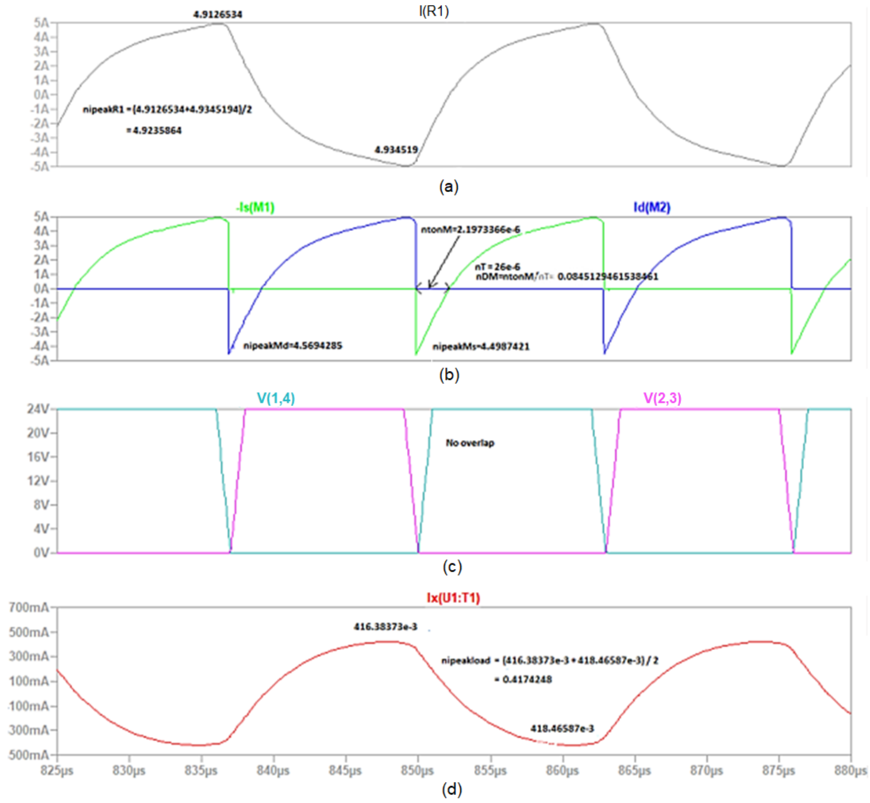

Fig. 12 The output waveforms for tuned transformer circuit, (a) current in R1, (b) current in MOSFET, (c) voltage at V(1,4) and V(2,3) and (d) current at load

Table 1: Comparisons between Untuned and Tuned step-up transformer circuits performance

Parameter	*Step-up Transformer Secondary Circuit*	
	Untuned	*Tuned*
Conversion power loss, P_{lost}	*65.519W*	*12.153 W*
Output power, $P_{rms}(Load)$	*35.10 W*	*29.068 W*
Conversion power Efficiency	*35.10%*	*70.52%*
Output current, $I_{rms}(Load)$	*0.326 A*	*0.295 A*
Output Voltage, V_{rms} $(Load)$	*108.742V*	*98.489V*

4 CONCLUSION

A comparative analysis between the two circuits can be made based on a few significant parameters summarized in Table 1. First and foremost, the most distinctive observation is that P_{lost} obtained in the untuned step-up transformer circuit is much higher compared to the P_{lost} Obtained in the other circuit. Even though the output power of the load in these two circuits has not much difference, due to the significant margin distinction in the value of P_{lost}. It has affected the circuit's performance, and this assessment was made using the efficiency computation made at both circuits. The high rate of P_{lost} in the untuned circuit caused the circuit to have an efficiency rate of 35.10%; meanwhile, the low value of P_{lost} in the tuned circuit has incremented its efficiency rate to 70.52%. Both circuits have the approximate output power value range of 30–35 W, suitable for producing sufficient cavitation bubbles during cleaning.

REFERENCES

[1] Grieser et al., Sonochemistry and the Acoustic Bubbles. Elsevier, 2015, pp. 1-9.
[2] M. Stanga, Ultrasound Cleaning in Sanitation, Wiley-VCH Verlag GmbH & Co. KGaA, 2010, pp. 473-476.
[3] A. A. Busnaina and G. W. Gale, "Ultrasonic and Megasonic Particle Removal," Proc. Precision Cleaning, pp. 347-360, 1995.
[4] B. Kanegsberg and E. Kanegsberg, Handbook for Critical Cleaning; Applications, Processes, and Controls, 2nd ed. Boca Raton: CRC Press, an imprint of Taylor & Francis Group, 2011. https://doi.org/10.1201/b10858
[5] M. Cai, S. Zhao, and H. Liang, "Mechanisms for the enhancement of ultrafiltration and membrane cleaning by different ultrasonic frequencies," Desalination, vol. 263, no. 1-3, pp. 133-138, 2010. https://doi.org/10.1016/j.desal.2010.06.049
[6] R. Magarajan, S. Awad, and K. R. Gopi, "Megasonic Cleaning," Developments in Surface Contamination and Cleaning, pp. 31-62, 2011. https://doi.org/10.1016/B978-1-4377-7885-4.10002-8
[7] F. Duran and M. Teke, "Design and Implementation of an Intelligent Ultrasonic Cleaning Device," Intelligent Automation and Soft Computing, pp. 1-10, 2018. https://doi.org/10.31209/2018.11006161
[8] S. Athira and K. Deepa, "Solar powered ultrasonic cleaner," 2014 Annual International Conference on Emerging Research Areas: Magnetics, Machines and Drives (AICERA/iCMMD), pp. 1-6, 2014. https://doi.org/10.1109/AICERA.2014.6908245
[9] J. Marshal and K. Deepa, "Hybrid renewable energy system: Optimum design, control and maximum utilization with SIBB converter using DSP controller," 2014 Power and Energy Systems: Towards Sustainable Energy, 2014.
[10] K. M. C. Basa, K. P. S. Gomez, F. B. Navarro-Tantoco, A. S. Quinio, G. P. Arada, and C. B. Co, "Design of a varying ultrasonic frequency amplifier," TENCON 2012 IEEE Region 10 Conference, pp. 1-6, 2012. https://doi.org/10.1109/TENCON.2012.6412169
[11] J. Jittakort, J. Nimsontorn, B. Sirboonrueng, S. Chua-On, P. Pinpathomrat, and S. Chudjuarjeen, "A Class D Voltage Source Resonant Inverter for Ultrasonic Cleaning Application," 2018 International Conference on Engineering, Applied Sciences, and Technology (ICEAST). https://doi.org/10.1109/ICEAST.2018.8434484